ELSEVIER

Journal of Nuclear Materials 241–243 (1997) 349–352

journal of nuclear materials

Density threshold for plasma detachment in gas target

N. Ezumi [a,*], S. Mori [b], N. Ohno [a], M. Takagi [a], S. Takamura [a], H. Suzuki [c], J. Park [d]

[a] *Department of Energy Engineering and Science, Graduate School of Engineering, Nagoya University, Nagoya 464-01, Japan*
[b] *Department of Electrical Engineering, Graduate School of Engineering, Nagoya University, Nagoya 464-01, Japan*
[c] *National Institute for Fusion Science, Nagoya 464-01, Japan*
[d] *Plasma Physics Laboratory, Princeton University, Princeton, NJ 08543, USA*

Abstract

The simulated gas target divertor experiment has been performed to investigate the fundamental physics of plasma detachment in the linear plasma device, TPD-I, which has a high heat flux and high density plasma in steady state. The existence of a density threshold for plasma detachment was observed in our experiment. It is found that the electron–ion temperature relaxation process is a key to determine the density dependence of the plasma detachment.

Keywords: Divertor simulator; Detached plasma

1. Introduction

Heat flux flowing into the divertor plate has been assumed to be more than 20 MW/m^2 for the next generation of fusion reactors such as ITER. It is quite difficult to develop a new material withstanding such a high heat load for a long time. ITER EDA has been considering a possible removable of such a high plasma heat flux from the divertor plate by intensive plasma–neutral interactions (detached divertor type). These interactions will be accompanied by decreasing not only the plasma temperature but also its momentum and constitute plasma detachment. Matthews defines 'plasma detachment' as a phenomenon accompanied by a dropping of the plasma pressure along the magnetic field [1]. In tokamaks, plasma detachment has been observed in JET [2], ASDEX-U [3], DIII-D [4] etc. However, the detailed physics of detachment is not so clear. Studies on the plasma–gas interaction in terms of plasma detachment are urgently needed in support of divertor physics R&D. There exist several studies on the fundamental physics on the plasma detachment in linear plasma devices [5–8]. We have performed a simulated gas target divertor experiment in the linear plasma device TPD-I to investigate the plasma density dependence of detachment. In this paper, we report the density threshold for plasma detachment associated with electron–ion energy relaxation processes.

2. Experimental results

The TPD-I device has a glass vacuum vessel with 200 cm in length and 14 cm in diameter, and is equipped with 21 solenoidal magnetic coils which produce a flux density of 3 kG in steady state. Helium plasma is generated by a sophisticated dc discharge using a LaB_6 cathode, and electron density n_e can be controlled by changing the discharge current I_p [8]. Typical plasma parameters are the electron density $n_e < 1.5 \times 10^{19}$ m^{-3} and the electron temperature $T_e < 10$ eV. The plasma diameter is about 2 cm. The inset in Fig. 3 shows the schematic of experimental arrangement. The device has an orifice, with a diameter of 3 cm at the center of the vacuum vessel, in order to minimize the influence of a neutral gas feed on the dc discharge conditions. When the plasma is attached, the plasma is terminated by the water-cooled target plate, located at a distance 87 cm from the orifice. Target gas feeding is controlled with a mass flow controller. The gas inlets are located at a distance of 5 cm and 66 cm from the orifice, respectively. Neutral pressure P_n, measured with

* Corresponding author. Tel.: 81-52 789 4426; fax: 81-52 789 3944; e-mail: n-ezumi@echo.nuee.nagoya-u.ac.jp.

PII S0022-3115(96)00527-2

the capacitance manometer at 33 cm away from the orifice; can be controlled up to 25 mTorr. The n_e, T_e and space potential V_S are measured by two fast-scanned Langmuir probes designated 'downstream' and 'upstream', installed at a distance 20 cm and 53 cm from the target plate, respectively. Plasma heat load to the target plate can be obtained with the temperature rise of the cooling water.

The gas target experiment was performed by feeding the helium neutral gas into the vacuum vessel. Fig. 1 shows the radial profile of n_e and T_e measured with the 'downstream' probe at the discharge current $I \sim 67$ A, as a function of P_n. n_e and T_e at the center are found to be 1.3×10^{19} m^{-3} and 8 eV without neutral gas feeding as shown in Fig. 1(a). From now on, this plasma density n_e is referred to as n_{e0} where suffix 0 means the value without any additional neutral gas feeding. With an increase in P_n, T_e is found to be rapidly decreasing to less than 2 eV, and the radial profile is changed to peaked to hollow. On the other hand, n_e is found to be gradually decreasing after T_e becomes low, and the radial profile becomes flat. It should be noted that a decrease in T_e at the center, where n_e is high, is larger than that at the periphery of the plasma column. Above $P_n = 11$ mTorr, there is almost no heat flux onto the target plate and plasma disappears in front of the target. In our experiments, plasma detachment means no heat load to the target plate within experimental accuracy, so called, 'energy detachment'.

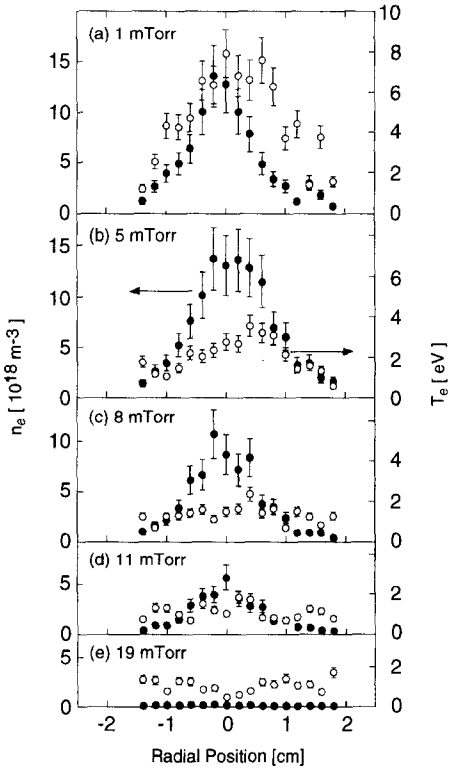

Fig. 1. Dependence of the radial profile of n_e and T_e in high n_{e0} case ($I_p \sim 67$ A). Neutral pressure P_n; (a) 1 mTorr, (b) 5 mTorr, (c) 8 mTorr, (d) 11 mTorr, (e) 19 mTorr. Closed and open circles show n_e and T_e, respectively.

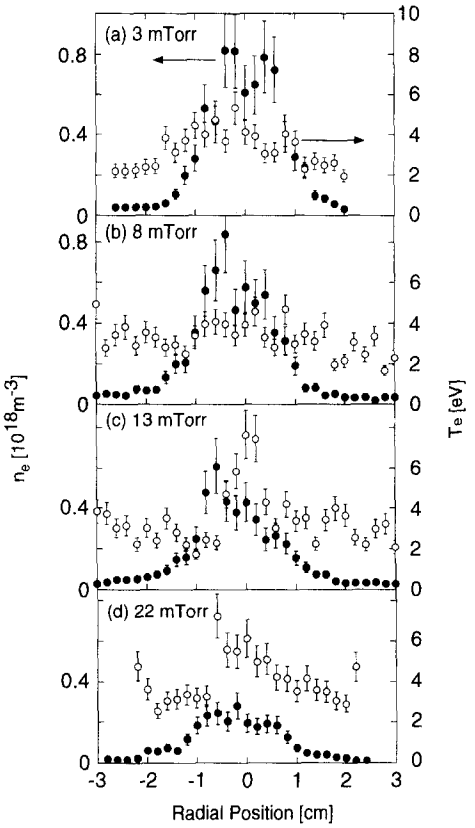

Fig. 2. Dependence of the radial profile of n_e and T_e in low n_{e0} case ($I_p \sim 10$ A). Neutral pressure P_n; (a) 3 mTorr, (b) 8 mTorr, (c) 13 mTorr, (d) 22 mTorr. Closed and open circles show n_e and T_e, respectively.

In the case of the low $n_{e0} \sim 0.8 \times 10^{18}$ m^{-3} ($I_p = 10$ A), P_n's dependence of the radial distributions of n_e and T_e are shown in Fig. 2. It is found that T_e is not changed so much by changing P_n from 3 mTorr to 22 mTorr, and n_e decreases by a factor of 4 at the center. Indeed, even in a high neutral pressure $P_n \sim 22$ mTorr, heat load to the target plate can be detected, and no plasma detachment is obtained at $n_{e0} \sim 0.8 \times 10^{18}$ m^{-3}. Fig. 3 shows the dependence of plasma pressure P, which is estimated as n_eT_e by meaning n_e and T_e at different positions along the magnetic field line, on the neutral pressure P_n. Furthermore, we note that the plasma pressure P is much larger than the neutral pressure P_n, in which the plasma detachment is observed. At a high plasma density $n_{e0} \sim 1.3 \times 10^{19}$ m^{-3}, the downstream plasma pressure is found to be decreasing more dramatically with an increase in P_n than that at upstream, as shown in Fig. 3(a). On the other hand, at $n_e \sim 2.0 \times 10^{18}$ m^{-3} ($I_p \sim 12$ A), P is gradually decreasing at both positions. Fig. 3(c) shows the ratio of P's at

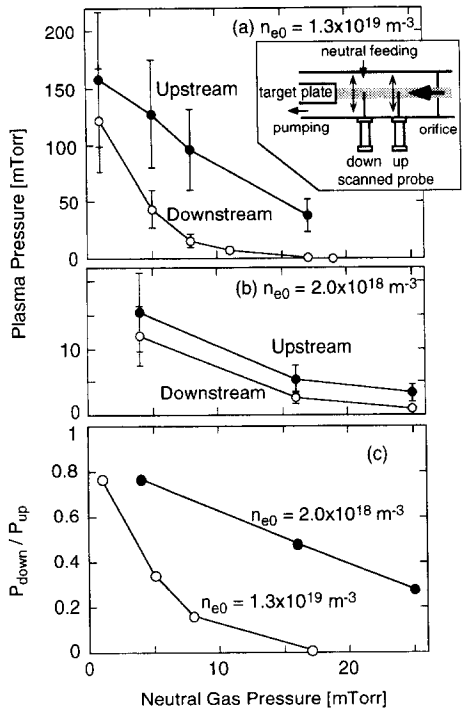

Fig. 3. Dependence of plasma pressure on neutral gas pressure P_n. The plasma pressure, to two different positions are estimated by the n_e and T_e measured with the scanned probes. (a) $n_{e0} \sim 1.3 \times 10^{19}$ m^{-3} ($I_p \sim 67$ A), (b) $n_{e0} \sim 2.0 \times 10^{18}$ m^{-3} ($I_p \sim 12$ A) and (c) the ratio of the plasma pressures measured at upstream and downstream.

downstream and upstream, which indicates that there is a steep plasma pressure drop only in the high plasma density $n_{e0} \sim 1.3 \times 10^{19}$ m^{-3}. The heat flux reduction rate Q/Q_0's as a function of n_e is shown in Fig. 4, where Q means the heat flux to the target plate. The Q/Q_0 is found to have the strong n_e's dependence at any P_n's. The experimental result that Q/Q_0 is substantially increasing with a decrease in n_e, shows that the plasma cooling effect by the neutral gas becomes weak at lower plasma density. Fig. 5

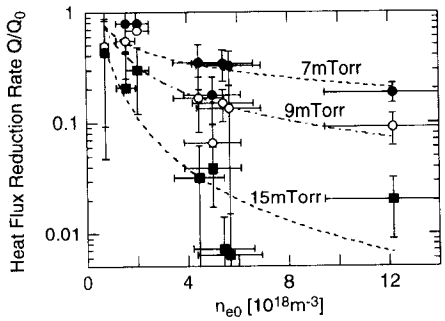

Fig. 4. Heat flux reduction rate as a function of n_{e0}, where Q_0 means the heat load to the target plate without the gas feeding.

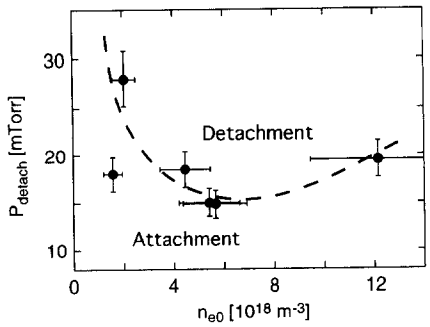

Fig. 5. Threshold values of the neutral pressure for the plasma detachment as a function of n_{e0}.

shows n_e's dependence of the neutral pressure: P_{detach}, at which plasma detachment occurs. As decreasing n_{e0}, the threshold value of P_{detach} is found to be rapidly increase, and below $n_e \sim 1.6 \times 10^{18}$ m^{-3}, plasma detachment is not observed in our experimental condition. This result indicates that there is the plasma density threshold for a generation of the plasma detachment.

3. Discussion

The density dependence on the plasma detachment is found in our experiments. In order to discuss this phenomena, we consider zero-dimensional electron and ion energy balance equations described as follows:

$$n_e V \frac{dT_e}{dt} = P_{in} - \frac{n_e(T_e - T_i)}{\tau_T^{ei}} V - n_e n_z \langle \sigma v \rangle_i E_i V - n_e n_z L_z V - \gamma_e T_e \Gamma_{wall} S \quad (1)$$

$$n_i V \frac{dT_i}{dt} = \frac{n_i(T_e - T_i)}{\tau_T^{ei}} V - n_i n_z \langle \sigma v \rangle_{cx} (T_i - T_z) - \gamma_i T_i \Gamma_{wall} S, \quad (2)$$

where P_{in} is the input power into plasma, $\langle \sigma v \rangle_i$ and $\langle \sigma v \rangle_{cx}$ are ionization and charge exchange rate coefficients, respectively, L_z is the power loss emission rate coefficient. E_i is the ionization potential. T_i and T_z are the ion temperature and the neutral temperature, respectively. S and V represent the surface area on the target plate where plasma is attached and the plasma volume. Γ_{wall} is the particle flux onto the target plate. γ_i and γ_e are the ion and the electron energy transmission factors through a sheath, respectively. τ_{ei} is the electron–ion temperature relaxation time given as follows:

$$\tau_T^{ei} = \frac{3\sqrt{2\pi}\,\pi\varepsilon_0^2 m_e^{-1/2} m_i T_e^{3/2}}{n_i Z_i^2 e^4 \ln \Lambda}, \quad (3)$$

where m_e and m_i are the electron and the ion masses, respectively. ε_0 is the permittivity of free space, Z_i is the

ionic charge number, e is the electron charge and ln Λ is the Coulomb logarithm. It should be noted that the e–i energy exchange is proportional to the square of plasma density. The reason why P_{in} exists in Eq. (1) is that the discharge power is thought to mainly input electrons in our experiment.

The electron energy loss mainly comes from ionization and radiation when T_e is more than 5 eV. However, at T_e less than 5 eV, electrons cannot lose their energy through the ionization and radiation processes, because the rate coefficient sharply decreases with decrease in T_e [9,10]. In our experiments as shown in Figs. 1 and 2, these processes are found not to be effective for cooling T_e, because T_e is usually less than 5 eV. Therefore, the energy exchange between electrons and ions becomes main electron energy loss channel instead of ionization and radiation since the e–i energy exchange time is proportional to $T_e^{3/2}$. On the other hand, the ions lose their energy by charge exchange and ion–neutral elastic collisions. When the electrons and ions are strongly coupled through the energy exchange process, the input power P_{in} to electrons can dissipate through the ions by the charge exchange process. In a low n_{e0} as shown in Fig. 2, the e–i coupling becomes weak. In fact, the estimation of τ_{ei}/τ_p indicates that in high n_{e0} ($\sim 10^{19}$ m^{-3}), the energy exchange sufficiently occurs due to small $\tau_{ei}/\tau_p \sim 0.29$, however in a low $n_{e0} \sim 10^{18}$ m^{-3}, τ_{ei}/τ_p becomes 2.6. The τ_p is the confinement time of plasma particles for axial direction defined by: $\sim L/0.2C_s$ where L is the length of plasma column (1.5 m) and $C_s \sim (T_e/m_i)^{1/2}$ is the ion sound velocity by using $T_e \sim 5$ eV and the factor 0.2 is determined by the results of the 2D fluid simulation comparing to our experiments [11]. If the τ_p is estimated by taking into account of the flux limited condition, the factor is not so change. Because the flux limited factor is 0.21 usually used. From the above discussions, the energy balance of plasma is shown schematically in Fig. 6. In the case of high n_{e0}, corresponding to Fig. 1, energy flux flows along the thick lines in Fig. 6. On the other hand, in low n_{e0}, this channel disappear because of the weak e–i coupling, so that there is no plasma detachment observed in our experiment. It comes from the fact that the electron energy is mainly lost through the ions by the energy exchange between electrons and ions finally to neutrals. Detailed modeling for our experiment has been done by using 2-dimension fluid code (B2 code). The simulation results corresponding to the Fig. 1, shows that ionization energy loss $\sim 22.8\%$ of total energy input and charge exchange energy loss $\sim 73.6\%$. On the other hand for Fig. 2, ionization energy loss $\sim 43.6\%$ and charge exchange energy loss $\sim 10.4\%$ are obtained. These simulation results are qualitatively in an agreement with the above discussion.

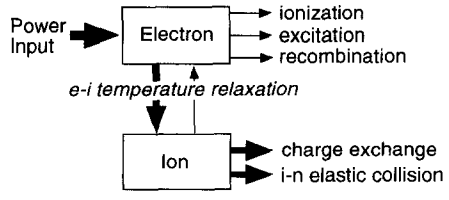

Fig. 6. Energy flow diagram in electrons and ions for explaining the density dependence of plasma detachment.

4. Conclusion

We have performed the gas target simulated experiments in the TPD-I device. Dependence of plasma detachment on plasma density is clearly demonstrated in our experiments. The density threshold is found to be associated with the electron–ion energy exchange process.

Acknowledgements

We thank Professor S.A. Cohen for reading the manuscript. This works was supported by the Japan-US collaboration program in the fusion area, the collaboration with the National Institute for Fusion Science (NIFS) in Japan and the Grant-in-Aid for Overseas Scientific Survey (contract No. 07044140), the Grant-in-Aid for Co-operative Research (contact No. 07308039) and Grant-in-Aid for Scientific Research (contact No. 07458113) from Japan Ministry of Education, Science and Culture.

References

[1] G.F. Matthews, J. Nucl. Mater. 220–222 (1995) 104.
[2] S. Clement et al., APS-DPP, Tampa, USA, 1991, JET IR (1991) 11.
[3] O. Gruber et al., Phys. Rev. Lett. 74 (1995) 4217.
[4] T.W. Petrie et al., J. Nucl. Mater. 196–198 (1992) 848.
[5] W.L. Hsu et al., Phys. Rev. Lett. 49 (1982) 1001.
[6] L. Schmitz et al., J. Nucl. Mater. 196–198 (1992) 841.
[7] G.S. Chiu and S.A. Cohen, Phys. Rev. Lett. 76 (1996) 1248.
[8] N. Ohno et al., J. Nucl. Mater. 220–222 (1995) 279.
[9] R.K. Janev et al., Elementary Processes in Hydrogen–Helium Plasmas (Springer-Verlag, 1987).
[10] T. Kato et al., Comparison of Ionization Rate Coefficients of Ions from Hydrogen through Nickel Reports of National Institute for Fusion Science, NIFS-DATA-14 (1991).
[11] N. Ohno et al., Contrib. Plasma Phys. 36 (1996) 339.